Prediction of clinical outcome after stereotactic body radiotherapy for non-small cell lung cancer using diffusion-weighted MRI and (18)F-FDG PET.

AUTHOR(S):

Iizuka, Yusuke; Matsuo, Yukinori; Umeoka, Shigeaki; Nakamoto, Yuji; Ueki, Nami; Mizowaki, Takashi; Togashi, Kaori; Hiraoka, Masahiro

CITATION:

Iizuka, Yusuke ...[et al]. Prediction of clinical outcome after stereotactic body radiotherapy for non-small cell lung cancer using diffusion-weighted MRI and (18)F-FDG PET.. European journal of radiology 2014, 83(11): 2087-2092

ISSUE DATE:

2014-11

URL:

http://hdl.handle.net/2433/191234

Abstract

Purpose/Objectives

To evaluate the use of diffusion-weighted magnetic resonance imaging (DW-MRI) and ^{18}F-fluorodeoxyglucose (FDG) positron emission tomography (PET) for predicting disease progression (DP) among patients with non-small cell lung carcinoma (NSCLC) treated with stereotactic body radiotherapy (SBRT).

Materials/Methods

Fifteen patients with histologically confirmed stage I NSCLC who underwent pre-treatment DW-MRI and PET and were treated with SBRT were enrolled. The mean apparent diffusion coefficient (ADC) value and maximum standardised uptake value (SUV_{max}) were measured at the target lesion and evaluated for correlations with DP.

Results

The median pre-treatment ADC value was 1.04×10^{-3} (range $0.83–1.29 \times 10^{-3}$) mm^2/s, and the median pre-treatment SUV_{max} was 9.9 (range 1.6–30). There was no correlation between the ADC value and SUV_{max}. The group with the lower ADC value ($\leq 1.05 \times 10^{-3}$ mm^2/s) and that with a higher SUV_{max} (≥ 7.9) tended to have poor DP, but neither trend was statistically significant ($p = 0.09$ and 0.32, respectively). The

combination of the ADC value and SUV_{max} was a statistically significant predictor of DP ($p = 0.036$).

Conclusion

A low ADC value on pre-treatment DW-MRI and a high SUV_{max} may be associated with poor DP in NSCLC patients treated with SBRT. Using both values in combination was a better predictor.

Introduction

Surgery is widely accepted as a standard therapy for stage I non-small cell lung cancer (NSCLC); however, some patients with stage I NSCLC are not suited for resection mainly because of their poor respiratory function.

Stereotactic body radiotherapy (SBRT) has recently been accepted as an alternative therapy for patients with stage I NSCLC who cannot undergo surgery or decline surgery [1-3]. In a previous study, medically inoperable patients were treated with peripheral T1-T2N0M0 NSCLC using SBRT [4]; the authors reported 3-year local control rates of 97.6% in a group of 55 patients with a median follow-up of almost 3 years, but distant metastasis was 22.1%. We previously reported a 3-year local control rate of 86.8% and a progression-free rate of 59.2% [5].

Histological findings are important factors for the determination of a treatment strategy and to predict clinical outcomes [6]. In lung SBRT, pathological diagnosis is confirmed in most patients before treatment is administered, however some patients undergo the treatment without histological confirmation due to the risk of adverse events caused by biopsy. Simple and less-invasive alternative methods are needed to stratify patients according to risk of disease progression (DP).

Advances in imaging technologies such as diffusion-weighted magnetic resonance imaging (DW-MRI) and ^{18}F-fluorodeoxyglucose (FDG) positron emission tomography (PET) have made it possible to evaluate not only morphological aspects, but also

functional aspects including diffusion motion of water molecules and glucose metabolism in tumours. These recently developed imaging techniques are applied to improve the sensitivity of tumour detection and prediction accuracy of the clinical outcomes. Several studies have analysed the utility of FDG-PET for the prognosis and prediction of therapeutic effect after treatment of NSCLC [7-9]. The apparent diffusion coefficient (ADC) of a tumour based on DW-MRI has been reported to be a useful indicator for early prediction of tumour response and prognosis in other cancers treated with chemoradiotherapy [10, 11]. To date, no study has evaluated the use of DW-MRI as a predictor for NSCLC treated with SBRT. Several studies have found that PET might be a useful predictor for patients with early-stage NSCLC treated with SBRT, but the results are controversial [12-15].

In this study, we evaluated whether pre-treatment DW-MRI and PET could be used to predict the clinical outcome of stage I NSCLC outcomes after SBRT and compared their predictive capabilities in the same tumours.

Materials/Methods

Subjects

The eligibility criteria for lung SBRT in our hospital were as follows: (1) T1a-T2aN0M0 lung tumour, (2) inoperable or refusal to undergo surgery, (3) arms could be held over the head for 30 min or more, and (4) performance status of 0–2.

Fifteen patients with histologically confirmed NSCLC who underwent pre-treatment DW-MRI and FDG-PET and were treated with SBRT in our hospital between January and December of 2010 were included this study. This study was approved by our Institutional Review Board. The median age was 80 years (range, 70–86 years). Eleven patients were male and four were female. Patients were staged according to the Union for International Cancer Control's TNM classification, 7th edition with CT and FDG-PET. Contrast medium was administered in the CT scan, if possible. The mean diameter of the tumours was 28 mm (range, 14–42 mm). T stages were distributed as follows: T1a in four, T1b in six, and T2a in five patients. Histological examinations included transbronchial biopsy (10 patients) or percutaneous CT-guided biopsy (5 patients) and were conducted before the pre-treatment DW-MRI and FDG-PET. The median interval between the biopsy and these imaging was 43 days (range, 17–67 days). The detailed characteristics of all patients are shown in Table 1.

SBRT procedure

The details of the SBRT procedure were described previously [16]. The patient's body was immobilised with an individualised vacuum pillow (BodyFIX; Elekta AB, Stockholm, Sweden). The SBRT protocol was created with a commercial treatment planning system, iPlan (BrainLab, Feldkirchen Germany). Four-dimensional computed tomography (4DCT) data were acquired in axial cine mode using a 16-slice CT scanner

(LightSpeed RT16, GE Healthcare, Waukesha, WI, USA) and real-time positioning management system (Varian Medical Systems, Palo Alto, CA, USA). An internal target volume (ITV) was determined by assessing tumour trajectory using 4DCT and tumour motion by X-ray fluoroscopy. Both techniques were employed because 4DCT is only capable of evaluating one respiratory cycle, and X-ray fluoroscopy can be used to evaluate the changes of tumour motion amplitude and duration of the respiratory cycle in several respiratory cycles. Planning target volume (PTV) was defined as ITV + margin (5mm).

Irradiation was performed with 6 MV X-ray beams from a linear accelerator (Novalis BrainLab) in multiple coplanar and noncoplanar static ports (6 to 8 ports). The dose was prescribed to the isocentre and dose distribution in PTV was homogeneous. The 70%-80% isodose lines encompassed the PTV edge. Dose distribution was calculated with the X-ray Voxel Monte Carlo method.

Prescribed doses and fractions were 48 Gy/4 fr (biologically effective dose [BED] of 105.6 Gy_{10}) for T1a-T1b, 56 Gy/4 fr (BED 134.0 Gy_{10}) for T2a, and 60 Gy/8 fr (BED 105.0 Gy_{10}) for centrally located tumours within 2 cm of the trachea or proximal bronchial tree, great vessels, and other mediastinal structures, regardless of their size. Overall treatment time was 4 to 11 days.

MRI protocol

All MRI examinations were performed using a 1.5T MR unit (Avanto, Siemens, Erlangen, Germany) with a phased-array coil. All patients were imaged in the supine position. Initially, transverse HASTE images were obtained for anatomical identification. Subsequently, both T2-weighted (TR/TE = 2100/85 ms) and DW-MR images with prospective acquisition correlation (PACE) utilising sensitivity encoding (SENSE; with a SENSE factor of 2) and echo planar imaging (EPI; with an EPI factor of 96) were obtained. The parameters used for DW-MRI were a TR/TE of 2746.3–12030.4/72–79 ms, FOV of 320 mm, slice thickness of 4.0 mm, matrix of 96 × 128 mm, band width of 1860 Hz/pixel and five excitations. All DW-MR images were acquired with MPG pulses in three directions (the x, y, and z axes) with three different b-factors (0, 500, and 1000 s/mm^2). All MR images covered the entire chest. ADC maps were automatically calculated from a series of DW images according to a linear regression model based on the logarithm of signal intensities as follows:

$$ADC = (\log SI_1/SI_0)/b$$

where SI_1 is the signal intensity with a diffusion gradient, SI_0 is the signal intensity without a diffusion gradient, and b is the gradient factor of sequences.

The ADC values of each tumour were measured by a single observer (SU) with 10 years of experience in clinical chest MRI. The mean signal intensity of the tumour was measured on an ADC map within three different circular regions of interest (ROIs) that were as large as possible. The average of these was calculated as the ADC value of the

126 tumour. All ROIs were established in the centre of the tumour to avoid artefacts from the
127 tumour/air interface or from blood flow in the surrounding large vessels. T2-weighted MR
128 images were also used as a reference, to avoid inclusion of necrotic areas in the ROIs. The
129 respiratory gating method was used for the MRI scan.
130
131 FDG-PET protocol
132 Patients fasted for at least 4 h before the examination, and their plasma glucose
133 level was checked immediately before the administration of ^{18}F-FDG (~3.7 MBq/kg). No
134 patients had a plasma glucose level greater than 200 mg/dL. Approximately 1 h later,
135 PET/CT was performed, using a combined PET/CT scanner (Discovery ST Elite, GE
136 Healthcare Waukesha, WI, USA). Low-dose CT images were acquired during shallow
137 breathing from the upper thigh to the skull base with a 16-detector row scanner (20–100
138 mA, using the auto-mA setting with a noise index of 30, 120 kV, 0.6 s tube rotation, slice
139 thickness 3.75 mm, matrix 512×512, and a pitch of 1.75). Immediately after CT, a
140 whole-body PET emission scan was performed in 3D-acquisition mode with an
141 acquisition time of 2–3 min per bed position. The PET images were attenuation-corrected
142 using the CT data and were reconstructed with a 3D ordered-subsets expectation
143 maximisation algorithm. The respiratory gating method was not used for the PET scan.
144 The maximum standardised uptake values (SUV_{max}) were measured at the target lesion by
145 a single observer (YN) with more than 10 years of experience in nuclear medicine.

146

147 Follow-up

148 Follow-up visits were conducted at 1, 2, 3, 6, 9, and 12 months in the first year
149 after SBRT and every 3–6 months thereafter. The plain CT scan was performed every 3
150 months in the first year after treatment and every 3–6 months thereafter. When DP was
151 highly suspected by the CT scan, FDG-PET was also performed.

152 Local progression (LP) was diagnosed based on the recommendations for
153 follow-up imaging established by Huang et al. [17]. Regional lymph node metastases
154 were diagnosed based on CT. FDG-PET results were also considered in diagnosis but
155 histological confirmation was not mandatory. DP was defined as LP, regional lymph node
156 metastases, or distant metastases.

157

158 Statistical analysis

159 The correlation of ADC value and SUV_{max} with DP after SBRT was evaluated. LP
160 and overall survival (OS) were evaluated in the same manner. To consider the impact that
161 the tumour diameter gives the ADC value and SUV_{max}, the correlations of ADC value and
162 SUV_{max} with tumour size were also evaluated. The cumulative incidence of DP and LP
163 was evaluated considering competing risk of non-lung cancer death. The Kaplan–Meier
164 method was used to estimate OS and the Grey-box test and log-rank test were used to
165 detect differences between strata. A p-value < 0.05 was considered statistically significant.

Receiver operating characteristic (ROC) analyses were performed to determine appropriate thresholds of ADC value and SUV_{max}. All statistical analyses were performed with R software (version 2.15.1, R Development Core Team)[18].

Results

Survival

The median follow-up period was 28.0 (range, 6.7–37.2) months. DP was observed in nine patients. The first site of progression was local tumour in three patients, regional lymph node in two patients, and distant metastasis in four patients. Seven of the nine DP were diagnosed with CT and FDG-PET. The remaining two patients who developed lung metastases were diagnosed with plain CT.

The OS at 24 months was 52% (seven patients died, 95% confidence interval [CI], 26–74%). The cumulative incidence rates of LP and DP were 16% (two patients) and 57%, (nine patients) respectively, at 24 months.

ADC value and SUV_{max}

The pre-treatment ADC values ranged from 0.83 to 1.29 × 10^{-3} mm^2/s (median 1.04 × 10^{-3} mm^2/s), and SUV_{max} ranged from 1.5 to 30.0 (median 9.9). There was no statistically significant correlation between ADC value and SUV_{max} (Fig. 1). Fig. 2 shows the scatter plot of tumour diameter and ADC value and SUV_{max}. ADC value and SUV_{max} showed weak positive correlations with tumour diameter with correlation coefficients of

186 0.48 and 0.50, but without statistical significance (p = 0.64 and 0.63, respectively).
187 According to the ROC analysis the appropriate threshold values for DP were 1.05×10^{-3}
188 mm^2/s for ADC value and 7.9 for SUV_{max}.
189 When dividing the patients into two groups according to the threshold ADC value
190 of 1.05×10^{-3} mm^2/s, the group with the lower ADC value had worse DP compared to
191 patients with the higher ADC value (80% and 20%, respectively, at 24 months). There
192 was a similar tendency in the group with the higher SUV_{max} ($\geq$ 7.9) to have a poor DP
193 (60% and 40%, respectively, at 24 months). However, neither DP trend was statistically
194 significant. (p = 0.09, and 0.32, respectively).
195 As an exploratory analysis, a combination of ADC value and SUV_{max} with the
196 same threshold values was investigated. When patients were divided into two groups
197 (high-risk group: patients with ADC value $\leq 1.05 \times 10^{-3}$ mm^2/s and $SUV_{max} \geq 7.9$; and
198 low-risk group: all other patients), the numbers of patients were well balanced between
199 the groups (8 and 7 patients for the high- and low-risk groups, respectively). The high-risk
200 group had significantly worse DP (p = 0.036). The cumulative incidence rates of DP were
201 75.0% (six patients) in the high-risk group and 28.6% (two patients) in the low-risk
202 groups, respectively, at 24 months (Fig. 3). The two groups had a similar number of
203 patients, and similar characteristics (Table 2).
204 The OS at 24 months was 50% (four patients died) in the high-risk group and 57%
205 (three patients died) in the low-risk group. However, from the viewpoint of cancer specific

death, the survival rates were 60% (three patients died) in the high-risk group and 83% (one patient died) in the low-risk group. The cumulative incidence rates of LP at 24 months were 14% (one patient) in both groups. The tumour diameter, pre-treatment ADC value and SUV_{max} of the patient in the high-risk group were 28 mm, 1.04×10^{-3} mm^2/s and 7.9. Those of the patient in the low-risk group were 42 mm, 1.19×10^{-3} mm^2/s and 13.6, respectively.

Discussion

To the best of our knowledge, this is the first study to evaluate the use of DW-MRI for predicting the clinical outcomes in NSCLC patients treated with SBRT. It is also the first direct comparison of FDG-PET and DW-MRI in terms of prognosis prediction for NSCLC patients who have undergone SBRT.

We found that patients presenting with stage I NSCLC and either a lower ADC value, or with a higher SUV_{max} tended to have a poor DP after SBRT although the difference was not statistically significant. The use of ADC value and SUV_{max} in combination was a better predictor for DP than either biological marker alone.

Several previous studies on PET in NSCLC patients treated with SBRT have been published. Various controversial results have been reported regarding the use of FDG-PET for prognosis. In a recent study of 152 patients treated with SBRT of 40 to 60 Gy in five fractions, SUV_{max} was a significant predictor of OS, disease-free survival, and

LP [14], although this study included patients with pathologically unconfirmed NSCLC. Another analysis showed that pre-treatment SUV_{max} was a significant predictor for disease-free survival and distant failure in 82 patients [12]. Burdick et al. evaluated the pre-treatment SUV_{max} in 72 patients treated with SBRT with a median follow-up of 16.9 months, however SUV_{max} did not predict OS and DP [15]. We found a correlation between SUV_{max} and DP, although there was no statistically significant correlation with DP.

The conventional PET scan has several problems for evaluation of SUV_{max}. First, the spatial resolution of the PET scanner is low. Second, the PET image is often blurred due to respiratory motion, especially in the lower lobes of the lung and upper abdominal organs. SUV_{max} is higher when measured using respiratory gating PET or CT reconstruction than when using conventional techniques in lung tumours [19]. If we had used the respiratory gating method in this study, a significant difference might have been observed.

The use of DW-MRI for predicting the therapeutic effect and prognosis is also controversial. To date, no published study has addressed DWI in early-stage NSCLC patients treated with SBRT. A few reports have discussed DW-MRI and lung cancer treated with chemoradiotherapy. Ohno et al. reported a correlation between DW-MRI and PET in a study of 64 patients with locally advanced NSCLC (stage III) treated with conventional chemoradiotherapy. They found that higher ADC and SUV_{max} values were

significantly associated with poor prognosis. OS and progression-free survival of the two groups split at an ADC value of 2.1×10^{-3} mm^2/s, and a SUV_{max} of 10 showed a significant difference [20]. Several studies have suggested that the ADC value is a predictive factor for other organs. In a study that analysed 32 patients with hypopharyngeal or oropharyngeal squamous cell carcinoma who underwent pre-treatment DWI and definitive chemoradiotherapy, patients with a higher ADC value (more than median, 0.79×10^{-3} mm^2/s) had a significantly lower local control rate than patients with a lower ADC value [21]. In contrast, Micco et al. reported that lower average pre-treatment ADC values were associated with high-risk features such as International Federation of Gynaecology and Obstetrics (FIGO) stage and LN metastases [10]. In another study, a lower ADC value was associated with shorter cancer-specific survival in patients with upper urinary tract cancer treated only with surgery [11]. Our result of a lower ADC value being associated with a poor prognosis after SBRT is in agreement with the latter reports. Several factors may have caused the different results. First, these studies defined ADC value differently. Different measures may be used to define the ROI and evaluate the ADC values, for example, using a minimum ADC value, a mean ADC value, or histogram analysis, etc [22-24]. We used the mean ADC value and avoided the cystic and necrotic areas to not affect the ADC value of the tumour. Second, the cancer type, clinical stage, and treatment strategies were different between the studies.

Some negative correlations between ADC value and cell density have been observed in certain malignancies. Tumours with a lower ADC value are more likely to have viable proliferative cells, which are sensitive to chemotherapy and radiotherapy. Conversely, the presence of inflammatory changes, necrosis, and fibrosis influence ADC value, which is correlated with interstitial water content and low cell density in histological samples [25, 26]. The lower the ADC value, the more effective the chemotherapy and/or radiotherapy [10, 20, 27].

Tumour size, patient gender, and operability are other prognostic factors suggested for early stage NSCLC treated with SBRT [5, 28. 29]. Our results suggest that the functional imaging modalities such as DW-MRI and PET could be a good predictor of clinical outcomes.

A limitation of this study is that the sample size was small. We introduced internal fiducial markers to a part of lung cancer patients in October 2010 to improve tumour localization during SBRT. The fiducial markers were made of gold and were inserted into bronchiole near the tumour [30]. Then, we stopped patient enrolment into the present study because of a concern that the gold markers might spoil image quality of DW-MRI. Despite of the small number, the present study indicated pre-treatment DW-MRI could be a predictor for clinical outcomes. A future study is warranted to prospectively evaluate the additional role of DW-MRI to FDG-PET before lung SBRT.

The present study did not evaluate ADC values after SBRT. There are some studies investigating the use of DW-MRI for predicting therapeutic effect of chemoradiation by comparing ADC values before and after treatment. Liu et al reported the percentage ADC value change after 1 month correlated positively with size reduction after 2 months of chemoradiation in 17 patients with cervical cancer [27]. Another study reported the ADC value at the time of 20 Gy was significantly higher in responders compared to non-responders in 27 patients with primary clinical T4 oesophageal carcinoma treated with chemoradiation [31]. We are planning a study to evaluate usefulness of DW-MRI in evaluation of the tumour response after SBRT and in distinction of treatment-related change from recurrence.

The consideration of more intensive therapy to prevent disease progression especially in high-risk patient is warranted. For example, dose escalation such as peripheral dose prescription and heterogeneous distribution, or systemic chemotherapy. However, early stage NSCLC patients treated with SBRT are often elderly and cannot tolerate chemotherapy. Thus, dose escalation is considered an appropriate strategy.

Conclusion

A low ADC value on pre-treatment DW-MRI and higher SUV_{max} may be associated with DP in NSCLC patients after SBRT. The combined use of ADC value and SUV_{max} is a better predictor for DP.

304

305 **References**

306 [1] Grutters JP, Kessels AG, Pijls-Johannesma M, De Ruysscher D, Joore MA, Lambin
307 P. Comparison of the effectiveness of radiotherapy with photons, protons and
308 carbon-ions for non-small cell lung cancer: a meta-analysis. Radiother Oncol
309 2010;95(1):32-40.
310 [2] Onimaru R, Shirato H, Shimizu S, Kitamura K, Xu B, Fukumoto S, et al. Tolerance of
311 organs at risk in small-volume, hypofractionated, image-guided radiotherapy for
312 primary and metastatic lung cancers. Int J Radiat Oncol Biol Phys
313 2003;56(1):126-35.
314 [3] Onishi H, Shirato H, Nagata Y, Hiraoka M, Fujino M, Gomi K, et al.
315 Hypofractionated stereotactic radiotherapy (HypoFXSRT) for stage I non-small
316 cell lung cancer: updated results of 257 patients in a Japanese multi-institutional
317 study. Journal of thoracic oncology : official publication of the International
318 Association for the Study of Lung Cancer 2007;2(7 Suppl 3):S94-100.
319 [4] Timmerman R, Paulus R, Galvin J, Michalski J, Straube W, Bradley J, et al.
320 Stereotactic body radiation therapy for inoperable early stage lung cancer. JAMA
321 2010;303(11):1070-6.
322 [5] Matsuo Y, Shibuya K, Nagata Y, Takayama K, Norihisa Y, Mizowaki T, et al.
323 Prognostic factors in stereotactic body radiotherapy for non-small-cell lung cancer.
324 Int J Radiat Oncol Biol Phys 2011;79(4):1104-11.
325 [6] Rezaei MK, Nolan NJ, Schwartz AM. Surgical pathology of lung cancer. Seminars
326 in respiratory and critical care medicine 2013;34(6):770-86.
327 [7] Higashi K, Ueda Y, Arisaka Y, Sakuma T, Nambu Y, Oguchi M, et al. 18F-FDG
328 uptake as a biologic prognostic factor for recurrence in patients with surgically
329 resected non-small cell lung cancer. Journal of nuclear medicine : official
330 publication, Society of Nuclear Medicine 2002;43(1):39-45.
331 [8] Sunaga N, Oriuchi N, Kaira K, Yanagitani N, Tomizawa Y, Hisada T, et al.
332 Usefulness of FDG-PET for early prediction of the response to gefitinib in
333 non-small cell lung cancer. Lung Cancer 2008;59(2):203-10.
334 [9] Weber WA, Petersen V, Schmidt B, Tyndale-Hines L, Link T, Peschel C, et al.
335 Positron emission tomography in non-small-cell lung cancer: prediction of
336 response to chemotherapy by quantitative assessment of glucose use. J Clin Oncol
337 2003;21(14):2651-7.
338 [10] Micco M, Vargas HA, Burger IA, Kollmeier MA, Goldman DA, Park KJ, et al.
339 Combined pre-treatment MRI and 18F-FDG PET/CT parameters as prognostic
340 biomarkers in patients with cervical cancer. European journal of radiology 2014.

[11] Yoshida S, Kobayashi S, Koga F, Ishioka J, Ishii C, Tanaka H, et al. Apparent diffusion coefficient as a prognostic biomarker of upper urinary tract cancer: a preliminary report. European radiology 2013;23(8):2206-14.
[12] Clarke K, Taremi M, Dahele M, Freeman M, Fung S, Franks K, et al. Stereotactic body radiotherapy (SBRT) for non-small cell lung cancer (NSCLC): is FDG-PET a predictor of outcome? Radiother Oncol 2012;104(1):62-6.
[13] Hoopes DJ, Tann M, Fletcher JW, Forquer JA, Lin PF, Lo SS, et al. FDG-PET and stereotactic body radiotherapy (SBRT) for stage I non-small-cell lung cancer. Lung Cancer 2007;56(2):229-34.
[14] Takeda A, Sanuki N, Fujii H, Yokosuka N, Nishimura S, Aoki Y, et al. Maximum standardized uptake value on FDG-PET is a strong predictor of overall and disease-free survival for non-small-cell lung cancer patients after stereotactic body radiotherapy. Journal of thoracic oncology : official publication of the International Association for the Study of Lung Cancer 2014;9(1):65-73.
[15] Burdick MJ, Stephans KL, Reddy CA, Djemil T, Srinivas SM, Videtic GM. Maximum standardized uptake value from staging FDG-PET/CT does not predict treatment outcome for early-stage non-small-cell lung cancer treated with stereotactic body radiotherapy. Int J Radiat Oncol Biol Phys 2010;78(4):1033-9.
[16] Takayama K, Nagata Y, Negoro Y, Mizowaki T, Sakamoto T, Sakamoto M, et al. Treatment planning of stereotactic radiotherapy for solitary lung tumor. Int J Radiat Oncol Biol Phys 2005;61(5):1565-71.
[17] Huang K, Dahele M, Senan S, Guckenberger M, Rodrigues GB, Ward A, et al. Radiographic changes after lung stereotactic ablative radiotherapy (SABR)--can we distinguish recurrence from fibrosis? A systematic review of the literature. Radiother Oncol 2012;102(3):335-42.
[18] Team RdC. R: A Language and Environment for Statistical Computing. In: R Foundation for Statistical Computing, 2012
[19] van Elmpt W, Hamill J, Jones J, De Ruysscher D, Lambin P, Ollers M. Optimal gating compared to 3D and 4D PET reconstruction for characterization of lung tumours. European journal of nuclear medicine and molecular imaging 2011;38(5):843-55.
[20] Ohno Y, Koyama H, Yoshikawa T, Matsumoto K, Aoyama N, Onishi Y, et al. Diffusion-weighted MRI versus 18F-FDG PET/CT: performance as predictors of tumor treatment response and patient survival in patients with non-small cell lung cancer receiving chemoradiotherapy. AJR American journal of roentgenology 2012;198(1):75-82.
[21] Ohnishi K, Shioyama Y, Hatakenaka M, Nakamura K, Abe K, Yoshiura T, et al. Prediction of local failures with a combination of pretreatment tumor volume and apparent diffusion coefficient in patients treated with definitive radiotherapy for

hypopharyngeal or oropharyngeal squamous cell carcinoma. Journal of radiation research 2011;52(4):522-30.

[22] Heo SH, Shin SS, Kim JW, Lim HS, Jeong YY, Kang WD, et al. Pre-Treatment Diffusion-Weighted MR Imaging for Predicting Tumor Recurrence in Uterine Cervical Cancer Treated with Concurrent Chemoradiation: Value of Histogram Analysis of Apparent Diffusion Coefficients. Korean journal of radiology : official journal of the Korean Radiological Society 2013;14(4):616-25.

[23] Matoba M, Tonami H, Kondou T, Yokota H, Higashi K, Toga H, et al. Lung carcinoma: diffusion-weighted mr imaging--preliminary evaluation with apparent diffusion coefficient. Radiology 2007;243(2):570-7.

[24] Mori T, Nomori H, Ikeda K, Kawanaka K, Shiraishi S, Katahira K, et al. Diffusion-weighted magnetic resonance imaging for diagnosing malignant pulmonary nodules/masses: comparison with positron emission tomography. Journal of thoracic oncology : official publication of the International Association for the Study of Lung Cancer 2008;3(4):358-64.

[25] Manenti G, Di Roma M, Mancino S, Bartolucci DA, Palmieri G, Mastrangeli R, et al. Malignant renal neoplasms: correlation between ADC values and cellularity in diffusion weighted magnetic resonance imaging at 3 T. La Radiologia medica 2008;113(2):199-213.

[26] Sugahara T, Korogi Y, Kochi M, Ikushima I, Shigematu Y, Hirai T, et al. Usefulness of diffusion-weighted MRI with echo-planar technique in the evaluation of cellularity in gliomas. Journal of magnetic resonance imaging : JMRI 1999;9(1):53-60.

[27] Liu Y, Bai R, Sun H, Liu H, Zhao X, Li Y. Diffusion-weighted imaging in predicting and monitoring the response of uterine cervical cancer to combined chemoradiation. Clinical radiology 2009;64(11):1067-74.

[28] Baumann P, Nyman J, Hoyer M, Wennberg B, Gagliardi G, Lax I, et al. Outcome in a prospective phase II trial of medically inoperable stage I non-small-cell lung cancer patients treated with stereotactic body radiotherapy. J Clin Oncol 2009;27(20):3290-6.

[29] Dunlap NE, Larner JM, Read PW, Kozower BD, Lau CL, Sheng K, et al. Size matters: a comparison of T1 and T2 peripheral non-small-cell lung cancers treated with stereotactic body radiation therapy (SBRT). The Journal of thoracic and cardiovascular surgery 2010;140(3):583-9.

[30] Ueki N, Matsuo Y, Nakamura M, et al. Intra- and interfractional variations in geometric arrangement between lung tumours and implanted markers. Radiother Oncol 2014;110(3):523-8.

[31] Imanishi S, Shuto K, Aoyagi T, Kono T, Saito H, Matsubara H. Diffusion-weighted magnetic resonance imaging for predicting and detecting the

early response to chemoradiotherapy of advanced esophageal squamous cell carcinoma. Digestive surgery 2013;30(3):240-8.

Table 1. Patients' characteristics (n =15)

Sex (male/female)	11/4
Age (years), median (range)	80, (70–86)
Performance status 0/1	11/4
Operability	
Operable/Inoperable	7/8
Smoking status	
Never smoker/ex-smoker	2/13
Histology	
Adenocarcinoma/SCC/NSCLC nos	7/6/2
Size of tumour (mm), median (range)	30, (14–42)
T stage	
T1a/T1b/T2a	4/6/5
Location	
Peripheral/Central	9/6
RUL/RML/RLL/LUL/LLL	4/1/4/3/3
Prescribed dose	
48 Gy/56 Gy/60 Gy	5/4/6

Abbreviations: SCC = squamous cell carcinoma; NSCLC nos = non-small cell lung cancer, not otherwise specified; RUL = right upper lung; RML = right middle lung; RLL = right lower lung; LUL = left upper lung; LLL = left lower lung. T stage was revised according to the 7th edition of the TNM classification for lung cancer.

Table 2. Patients' characteristics in the high- and low-risk groups.

The high-risk group consisted of patients with an apparent diffusion coefficient (ADC) value $\leq 1.05 \times 10^{-3}$ mm^2/s and maximum standardised uptake values (SUV_{max}) ≥ 7.9. The other patients were in the low-risk group. The two groups were not different statistically.

	High-risk group (n = 8)	Low-risk group (n = 7)
Sex (male/female)	6/2	5/2
Age (years), median	72–86, 80	70–83, 80
Performance status 0/1	6/2	5/2
Operability		
Operable/Inoperable	4/4	3/4
Smoking status		
Never smoker/ex-smoker	0/8	2/5
Histology		
Adenocarcinoma/SCC/NSCLC nos	4/3/1	3/3/1
Size of tumour (mm), median (range)	28.5(17–35)	30(14–42)
T stage		
T1a/T1b/T2a	2/3/3	2/3/2
Prescribed dose		
48 Gy/56 Gy/60 Gy	3/2/3	2/2/3

Abbreviations: SCC = squamous cell carcinoma; NSCLC nos = non-small cell lung cancer, not otherwise specified. T stage was revised according to the 7th edition of the TNM classification for lung cancer.

Figures

Fig. 1. Scatter plot of the apparent diffusion coefficient (ADC) value and maximum standardised uptake (SUV_{max}). There was no statistical correlation between ADC value and SUV_{max} (r = 0.046).

Fig. 2. Scatter plot of the apparent diffusion coefficient (ADC) value and tumour diameter (A) and maximum standardised uptake (SUV_{max}) and tumour diameter (B). There was no statistical correlation (p=0.64 and 0.63, respectively).

Fig. 3. Cumulative incidence of disease progression (DP) according to apparent diffusion coefficient (ADC) value (A), maximum standardised uptake (SUV_{max}) (B), and the combination of ADC value and SUV_{max} (C). The group with the lower ADC value and higher SUV_{max} tended to have worse prognosis, although this result was not significantly significant (p = 0.09 and 0.32, respectively). When applying an optimal cut-off value of the ADC and SUV_{max}, the lower ADC value and higher SUV_{max} group had a significantly poorer prognosis (p = 0.036); the combination was a strong predictor for DP.

Figures

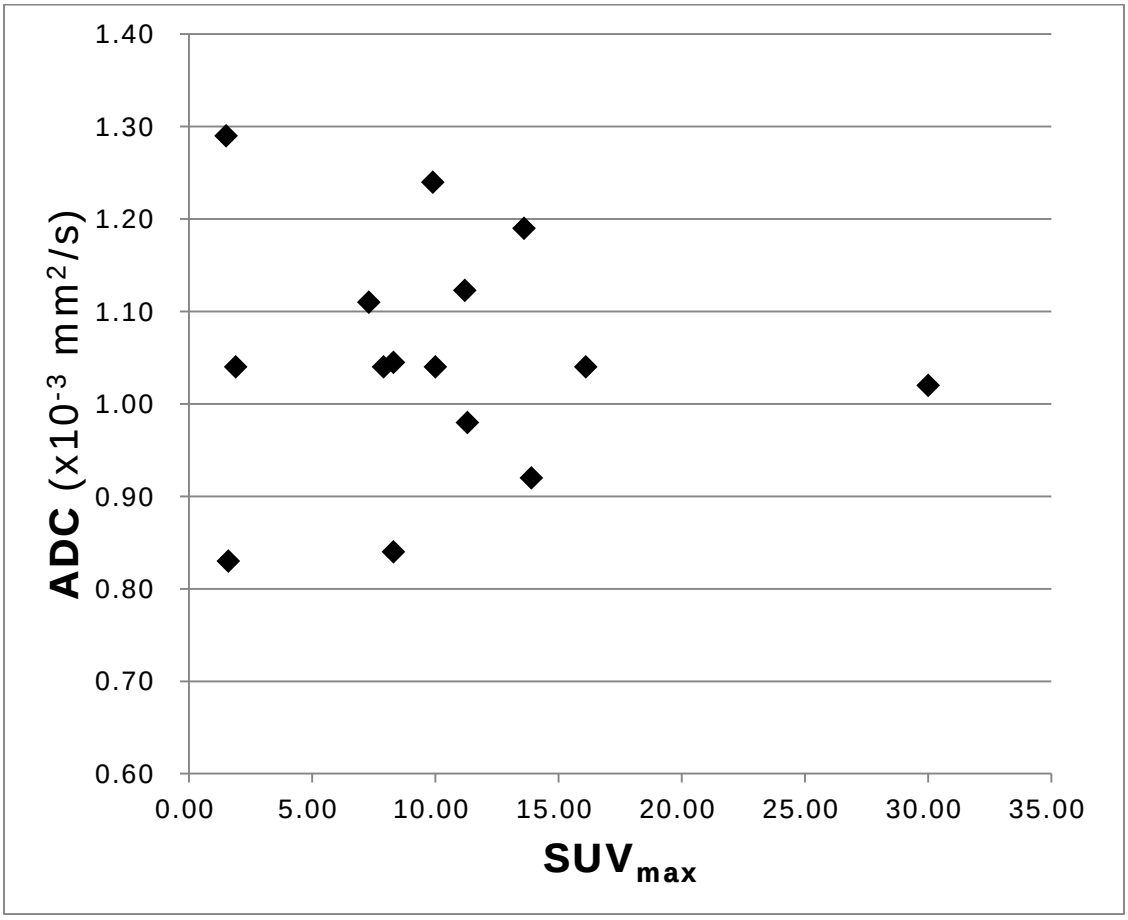

Fig. 1. Scatter plot of the apparent diffusion coefficient (ADC) value and maximum standardised uptake (SUV_{max}). There was no statistical correlation between ADC value and SUV_{max} (r = 0.046).

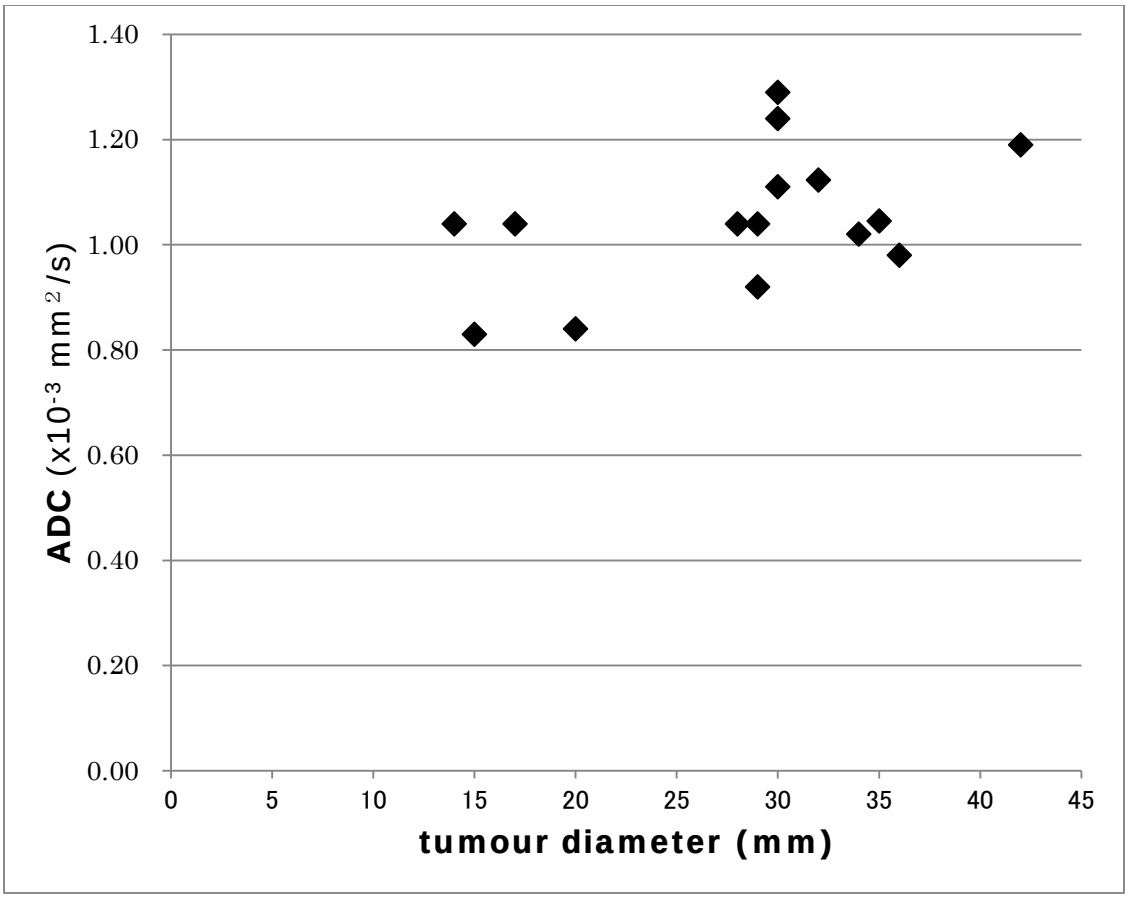

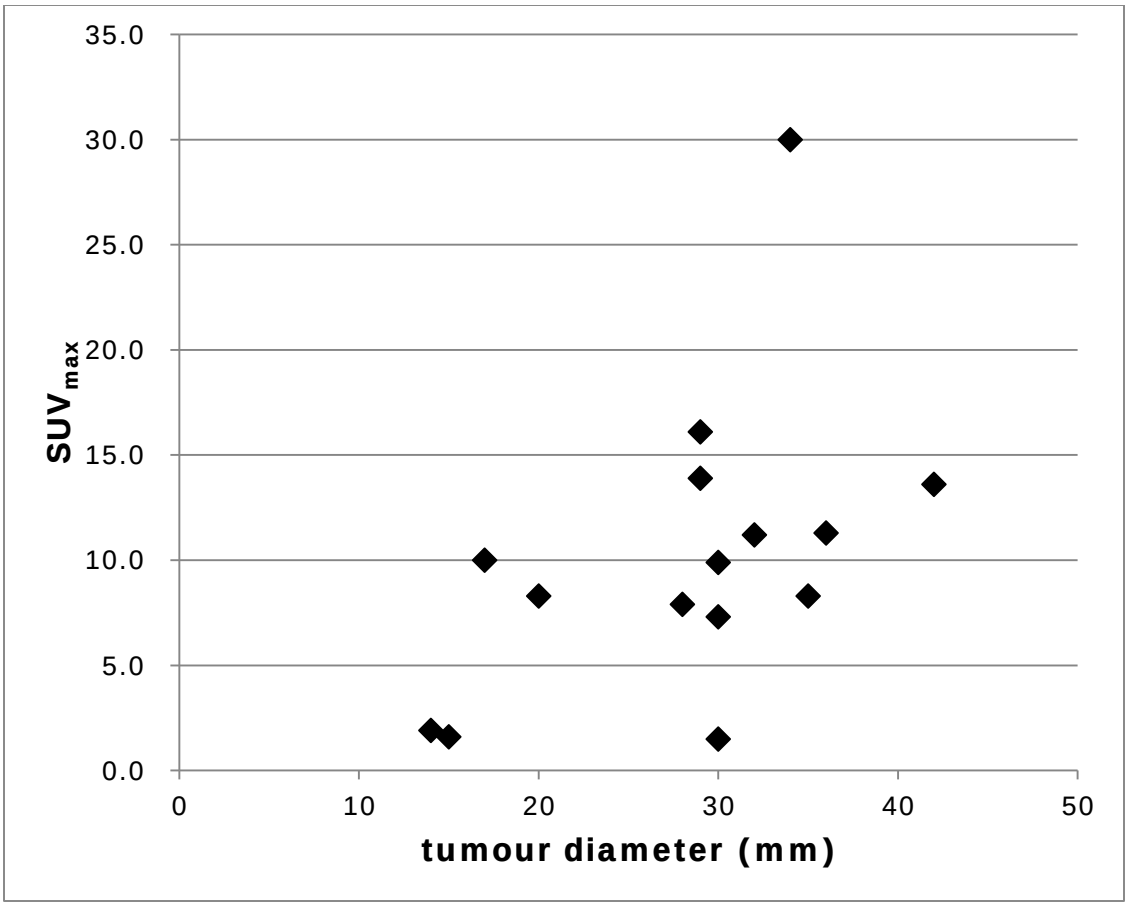

Fig. 2. Scatter plot of the (A) apparent diffusion coefficient (ADC) value and tumour diameter and (B) maximum standardised uptake (SUV_{max}) and tumour diameter. There was no statistical correlation (p=0.64 and 0.63, respectively).

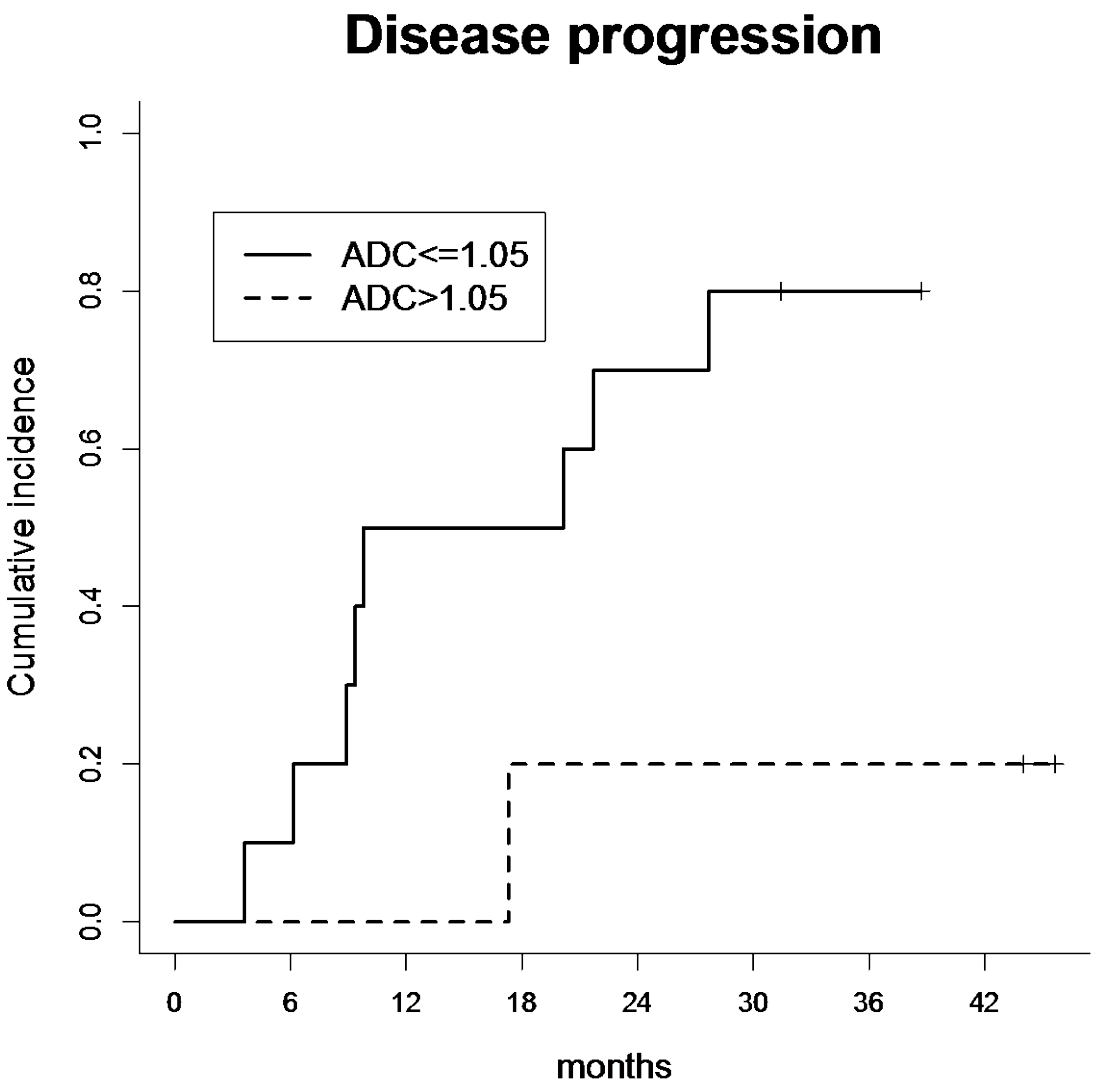

(A)

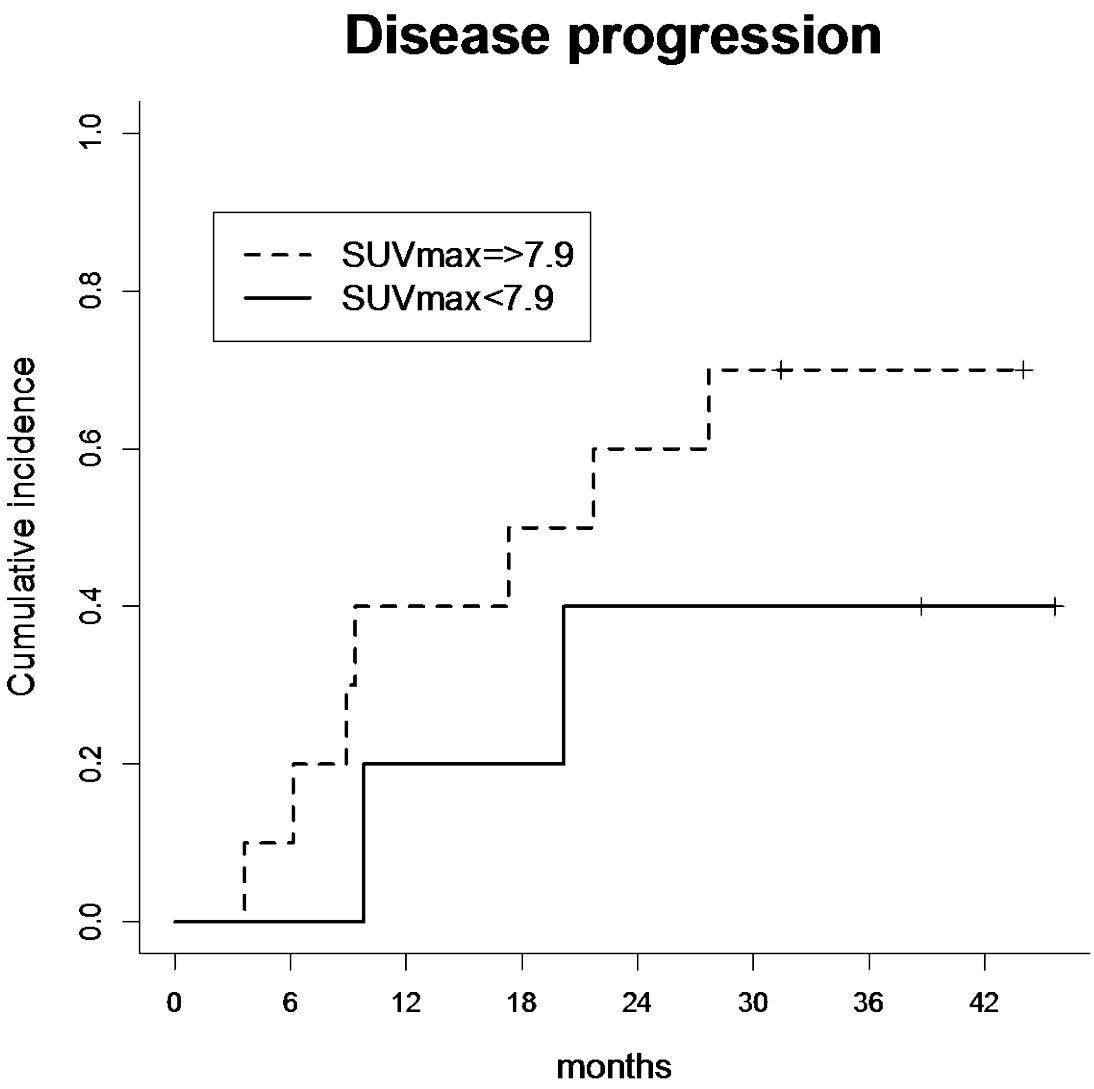

(B)

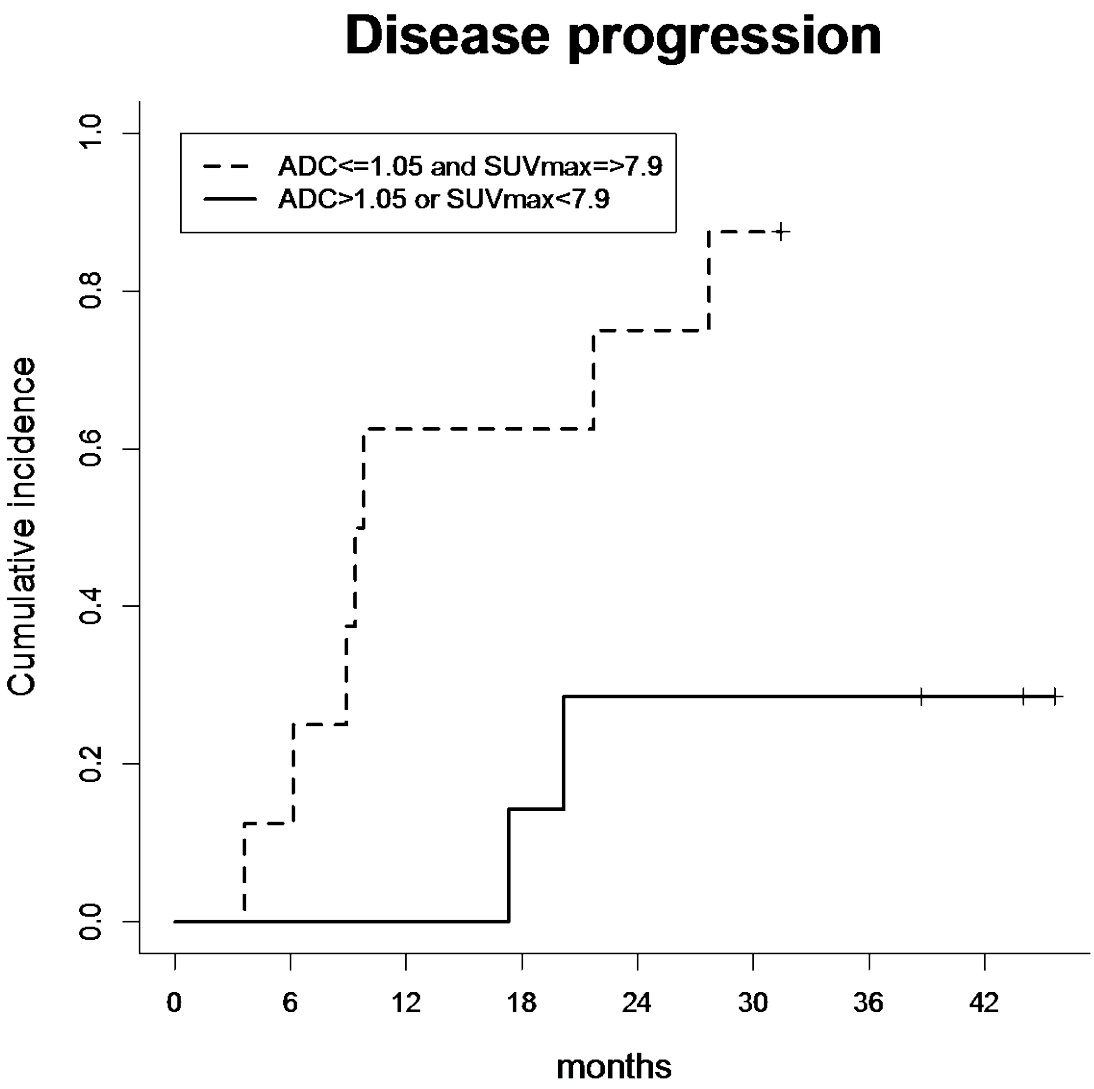

(C)

Fig. 3. Cumulative incidence of disease progression (DP) according to apparent diffusion coefficient (ADC) value (A), maximum standardised uptake (SUV_{max}) (B), and the combination of ADC value and SUV_{max} (C). The group with the lower ADC value and higher SUV_{max} tended to have worse prognosis, although this result was not significantly significant (p = 0.09 and 0.32, respectively). When applying an optimal cut-off value of

the ADC and SUV_{max}, the lower ADC value and higher SUV_{max} group had a significantly poorer prognosis ($p = 0.036$); the combination was a strong predictor for DP.